Electron Interactions With CF_3I

Cite as: Journal of Physical and Chemical Reference Data **29**, 553 (2000); https://doi.org/10.1063/1.1318910
Submitted: 09 November 1999 . Published Online: 05 March 2001

L. G. Christophorou, and J. K. Olthoff

Electron Interactions With CF_3I

L. G. Christophorou[a] and J. K. Olthoff[b]

Electricity Division, Electronics and Electrical Engineering Laboratory, National Institute of Standards and Technology, Gaithersburg, Maryland 20899-8113

Received November 9, 1999; revised version received July 26, 2000

Low-energy electron collision data for the plasma processing gas CF_3I are sparse. Limited cross section data are available only for total and differential elastic electron scattering, electron-impact ionization, and electron attachment. These data are assessed, synthesized, and discussed in this paper. There is a need for confirming measurements for some of these data, and for measurements of cross sections for the other main electron–collision processes for which no data exist. There are presently no data available for the electron transport, ionization, and attachment coefficients of this molecule. © *2001 by the U.S. Secretary of Commerce on behalf of the United States. All rights reserved.* [S0047-2689(00)00504-3]

Key words: attachment; CF_3I; coefficients; cross sections; electron interactions; electron transport; ionization; scattering; trifluoroiodomethane.

Contents

List of Tables

List of Figures

[a]Electronic mail: loucas.christophorou@nist.gov
[b]Electronic mail: james.olthoff@nist.gov

TABLE 1. Definition of symbols

Symbol	Definition	Common scale and units
$\sigma_{pa,t}(\lambda)$	Total photoabsorption cross section	10^{-19} cm^2; 10^{-23} m^2
$\sigma_{sc,t}(\varepsilon)$	Total electron scattering cross section	10^{-16} cm^2; 10^{-20} m^2
$\sigma_{e,diff}$	Elastic differential electron scattering cross section	10^{-16} cm^2 sr^{-1}
$\sigma_m(\varepsilon)$	Momentum transfer cross section (elastic)	10^{-16} cm^2; 10^{-20} m^2
$\sigma_{vib,diff}(\varepsilon)$	Vibrational differential electron scattering cross section	10^{-16} cm^2 sr^{-1}
$\sigma_{i,partial}(\varepsilon)$	Partial ionization cross section	10^{-16} cm^2; 10^{-20} m^2
$\sigma_{i,t}(\varepsilon)$	Total ionization cross section	10^{-16} cm^2; 10^{-20} m^2
$\sigma_{a,t}(\varepsilon)$	Total electron attachment cross section	10^{-14} cm^2; 10^{-18} m^2
$k_{a,t}(\langle\varepsilon\rangle)$	Total electron attachment rate constant	10^{-7} cm^3 s^{-1}
$(k_{a,t})_{th}$	Thermal electron attachment rate constant	10^{-7} cm^3 s^{-1}

1. Introduction

Trifluoroiodomethane (CF_3I) is a potential plasma etching gas (e.g., see Refs. 1–6) that provides copious quantities of CF_3^+ and CF_3 via dissociative electron-impact ionization and dissociative electron attachment. These reactive species play a key role in the plasma etching of Si and SiO_2. CF_3I is also an ''environmentally friendly'' gas as its overall atmospheric lifetime is very short (<1 to a few days).[7–9] Consequently, its global warming potential is very low (1–5 times that of CO_2).[7,10] This is in sharp contrast to the much higher global warming potentials of other plasma etching gases, such as the fully fluorinated hydrocarbons and SF_6.[10] Because of its short lifetime, CF_3I does not contribute significantly to ozone depletion.[7]

In this paper, as in the previous eight papers[11–18] in this series on electron interactions with plasma processing gases, we assess and synthesize the available information on the cross sections and rate coefficients for collisional interactions of electrons with CF_3I. Definitions of the symbols used here to describe the various collision processes discussed in the paper are given in Table 1.

2. Electronic Structure and Basic Properties

The trifluoroiodomethane (CF_3I) molecule belongs to the C_{3v} point group. It is polar, and McClellan[19] lists two values for its electric dipole moment: 0.92 D and (1.0 ± 0.1) D ($1\ \mathrm{D}=3.3356\times10^{-30}$ C m). Of its six fundamental vibrational frequencies $(\nu_1,\ldots,\nu_6)$, the ν_4, ν_5, and ν_6 are degenerate, and the ν_1, ν_2, and ν_4 are infrared active.[20] The ν_1, ν_3, and ν_4 frequencies have been attributed to stretching modes, ν_2, and ν_5 to deformation modes, and ν_6 to a bending mode. The energies of the six vibrational modes of CF_3I as given by Shimanouchi[20] are, respectively: 1080 cm^{-1} (0.134 eV), 742 cm^{-1} (0.092 eV), 286 cm^{-1} (0.035 eV), 1187 cm^{-1} (0.147 eV), 537 cm^{-1} (0.067 eV), and 260 cm^{-1} (0.032 eV) (see also Bürger *et al.*[21] for vibrational frequencies of $^{12}CF_3I$ and $^{13}CF_3I$).

The CF_3I molecule has a positive (adiabatic) electron affinity. Atom-impact crossed-molecular beam studies have provided values of the electron affinity (EA) of CF_3I. These are listed in Table 2 along with other pertinent fundamental data. The lowest unoccupied molecular orbital (LUMO) of CF_3I is an antibonding σ-type orbital of a_1 symmetry and is almost entirely localized on the C–I bond. The small dissociation energy D and relatively long length of the F_3C–I^- bond indicate that CF_3I^- can be regarded as a weakly bound radical anion.[22]

In Table 3 are listed the energy positions of the negative ion states of the CF_3I molecule, as they have been deter-

TABLE 2. Basic data on CF_3I and CF_3I^-

Physical quantity	Value	Reference/method
CF_3I		
Electron affinity	1.278 eV	22/Calculation
(adiabatic)	1.29±0.1 eV	23/Charge exchange in Cs–CF_3I collisions
	1.4±0.2 eV	24/Charge exchange in Cs–CF_3I collisions
	1.54±0.2 eV	25/Charge exchange in Na–CF_3I collisions
	1.6±0.2 eV	25/Charge exchange in Cs–CF_3I collisions
	2.2±0.2 eV	26/Charge exchange in K–CF_3I collisions
D (CF_3–I)	1.9 eV	27/Electron attachment using mass spectrometry
	2.0±0.2 eV	25/Charge exchange in Na–CF_3I collisions
	2.05±0.2 eV	24/Charge exchange in Cs–CF_3I collisions
	2.2±0.2 eV	26/Charge exchange in K–CF_3I collisions
	2.33±0.17 eV	28/Reaction kinetics
	2.39±0.04 eV	29/Photodissociation
	2.681 eV (2.4 eV)[a]	22/Calculation
R (C–I)	2.122±0.037 Å	30/Electron diffraction
	2.134±0.02 Å	31/Microwave spectroscopy
	2.135±0.033 Å	32/Electron diffraction
	2.137±0.032 Å	32/Electron diffraction
	2.140 Å	22/Calculation
	2.1438 Å	33/Microwave spectroscopy
R (C–F)	1.328±0.026 Å	30/Electron diffraction
	1.3285 Å	33/Microwave spectroscopy
	1.334±0.015 Å	32/Electron diffraction
	1.340±0.021 Å	32/Electron diffraction
	1.343 Å	22/Calculation
∠F–C–F	108.1°	22/Calculation
	108.2°±1.6°	32/Electron diffraction
	108.3°±2°	30/Electron diffraction
	108.4°±1.9°	32/Electron diffraction
	108.42°	33/Microwave spectroscopy
CF_3I^-		
D (CF_3–I^-)	0.29±0.2 eV	25/Charge exchange in Cs–CF_3I collisions
	0.35±0.2 eV	25/Charge exchange in Na–CF_3I collisions
	0.38±0.1 eV[b]	24/Charge exchange in Cs–CF_3I collisions
	0.610 eV	22/Calculation
R (C–I)	2.881 Å	22/Calculation
R (C–F)	1.367 Å	22/Calculation
∠F–C–F	106.0°	22/Calculation

[a]Roszak *et al.*[22] point out that the spin–orbit effect could be important in computing the bond dissociation energy and the electron affinity of the CF_3I molecule, since the $^2P_{3/2}$–$^2P_{1/2}$ splitting of the I atom is 0.94 eV. The value in parenthesis includes spin–orbit correction.
[b]Obtained using EA (I)=3.063 eV.

mined from electron scattering and electron attachment studies (see also Secs. 3 and 8). The presence of the dissociative electron attachment resonance near 0 eV indicates that the electron attachment cross section will be large at low energies, and thus suggests that the contribution of this process to the total electron scattering cross section will be substantial.

Figure 1 shows the total room-temperature photoabsorption cross section, $\sigma_{pa,t}(\lambda)$, of CF_3I as a function of the photon wavelength λ in the wavelength range 160–390 nm.[7,9,45,46] The spectrum consists of a continuous absorption band with a local maximum cross section value of about 6.0×10^{-19} cm^2 at 267 nm (4.64 eV). The absorption band is

TABLE 3. Energy positions of the negative ion states of the CF_3I molecule

Energy position (eV)	Reaction mechanism/Possible assignment	Reference and comments
0.0	$e+CF_3I \rightarrow I^- + CF_3$[a]	27, Electron attachment using mass spectrometry
0.0	$e+CF_3I \rightarrow I^- + CF_3$	35–37, Dissociative attachment producing I^-
0.0	$e+CF_3I \rightarrow I^- + CF_3$ $a_1(C-I\sigma^*)$	38, Total dissociative attachment cross section measurement[b]
~0.0	$e+CF_3I \rightarrow I^- + CF_3$	39, Total dissociative attachment cross section measurement[b]
0.4	$a_1(C-I\sigma^*)$	40, Calculation
~1.0	$e+CF_3I \rightarrow F^- + CF_2I$[c]	39, Total dissociative attachment cross section measurement
~1.5	$e+CF_3I \rightarrow F^- + CF_2I$	27, Electron attachment using mass spectrometry
1–2	$e+CF_3I^* \rightarrow F^- + CF_2I$	41, Formation of F^- from CF_3I at 500 and 700 K[d]
3.8	$e+CF_3I \rightarrow F^- + CF_2I$[e]	35, 36, Dissociative attachment producing F^-
3.8	$e+CF_3I \rightarrow CF_3^- + I$	35–37, Dissociative attachment producing CF_3^-
~4.5	$a_1(C-F\sigma^*)$	38, Total dissociative attachment cross section measurement
~4.9	$a_1(C-F\sigma^*)$ and $e(C-I\pi^*)$	40, Total electron scattering cross section measurement/Calculation
4–10	$a_1(C-F\sigma^*)$ and $e(C-I\pi^*)$	42–44, Vibrational excitation cross section function measurements

[a]Dibeler *et al.* in Ref. 34 give the onset of this process as ~0.0 eV, but the maximum intensity at the unacceptably high value of 1.8 eV.
[b]Due almost entirely to the respective reaction shown in column 2 of this table.
[c]Suggested possible reaction in Ref. 39.
[d]Found to be strongly temperature dependent.
[e]Dibeler *et al.* in Ref. 34 give a threshold value of 3.6±0.3 eV for this process, and a maximum-abundance energy of 5.6 eV.

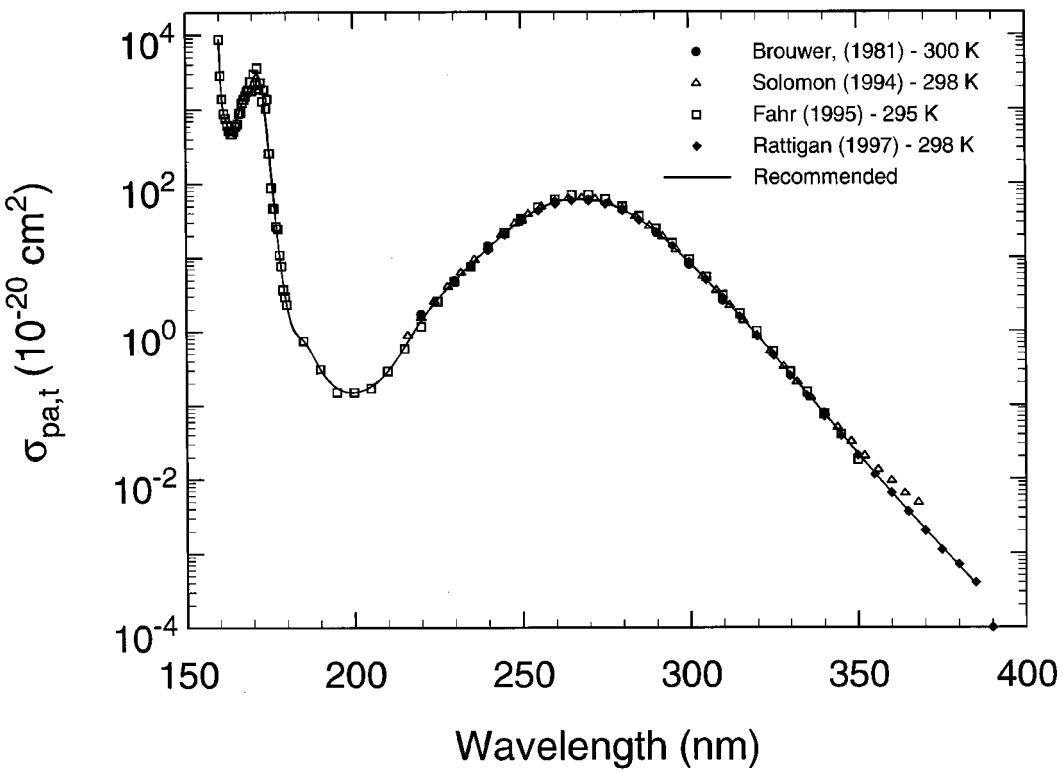

FIG. 1. Total photoabsorption cross section, $\sigma_{pa,t}(\lambda)$, as a function of the photon wavelength, λ, for CF_3I: (●) Ref. 45; (△) Ref. 7; (□) Ref. 46; (♦) Ref. 9.

TABLE 4. Recommended total photoabsorption cross section, $\sigma_{pa,t}(\lambda)$, for CF_3I in the wavelength range 160 nm to 385 nm ($T=295$ K to 300 K)

Wavelength (nm)	$\sigma_{pa,t}(\lambda)$ (10^{-20} cm^2)	Wavelength (nm)	$\sigma_{pa,t}(\lambda)$ (10^{-20} cm^2)
160	8716	230	4.81
161	1385	240	13.4
162	764	250	32.1
164	477	260	55.5
166	886	270	61.5
168	1529	280	44.3
170	2376	290	22.3
171	2905	300	8.52
173	1806	310	2.83
175	257	320	0.885
178	10.9	330	0.262
180	2.33	340	0.0764
185	0.75	350	0.0218
190	0.31	360	0.006 51
200	0.15	370	0.002 08
210	0.29	380	0.000 67
220	1.39	385	0.000 38

due to $n\rightarrow\sigma^*$ transitions involving excitation of a nonbonding p electron on the I atom to an antibonding σ^* orbital involving the C and I atoms[9] (see also Robin[47] and Herzberg[48]). Photoabsorption measurements have also been reported as a function of temperature.[7,9,45,46] Brouwer and Troe[45] made photoabsorption measurements at 300, 625, and 1050 K that show considerable band broadening at high temperatures. They also observed thermal decomposition of

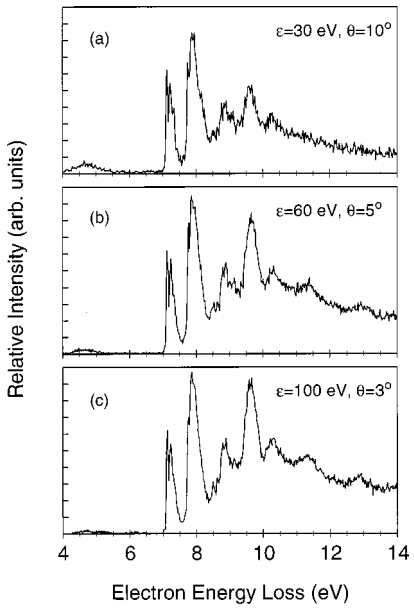

FIG. 2. Electron energy-loss spectrum of CF_3I for 30 eV (scattering angle of 10°), 60 eV (scattering angle of 5°), and 100 eV (scattering angle of 3°) incident-electron energies [data of Kitajima *et al.* from Ref. 43, as provided to the authors by Professor H. Tanaka (Ref. 44)].

TABLE 5. Threshold energies for the production of the parent and fragment positive ions by photon and electron impact on CF_3I

Positive ion	Threshold energy (eV)	Reference and method
CF_3I^+ ($X\,^2E_{3/2}$)[a,b]	10.23	50, 51, MSPI[c]
	10.29	52, 53
	10.32±0.03	54, ICR/PI[d]
	10.45	55, PES[e]
	10.61	56
	10.81	57, PES
	≤10.9[f]	58, EI[g]
CF_3I^+ ($X\,^2E_{1/2}$)	10.91	52, 53
	11.18	55, PES
	11.37	57, PES
CF_3^+	10.89	50, MSPI
	10.91[h]	59, DPI[i]
	11.36±0.03	54
	11.85[j]	59/DPI
	≤11.7	58, EI
$I^+(^3P_2)$	12.70	59, DPI
$I^+(^3P_0)$	13.50	59, DPI
$I^+(^3P_1)$	13.58	59, DPI
	≤14.5	58, EI
CF_2I^+	13.40	59, DPI
	≤14.3	58, EI
CF_2^+	17.62	59, DPI

[a]The CF_3I^+ ground state is a doublet, $X\,^2E_{3/2}$ and $X\,^2E_{1/2}$. The two states are separated by ~0.6 eV.
[b]Associated with the removal of a lone-pair electron from the I atom.
[c]MSPI=mass spectrometric photoionization study.
[d]ICR/PI=Ion cyclotron resonance/photoionization technique.
[e]PES=photoelectron spectra.
[f]The electron energy resolution was not adequate to allow separation of the $X\,^2E_{3/2}$ and $X^2E_{1/2}$ states of CF_3I^+.
[g]EI=electron impact.
[h]For the products $CF_3^+ + I(^2P_{3/2})$.
[i]DPI=dissociative photoionization.
[j]For the products $CF_3^+ + I(^2P_{1/2})$.

CF_3I at temperatures above ~1000 K (see also Ref. 49). The solid line in Fig. 1 is a least squares fit to the four sets of ''room temperature'' measurements. Values from this line are listed in Table 4 as the recommended $\sigma_{pa,t}(\lambda)$ for CF_3I.

Recent electron energy-loss spectra of CF_3I at 5° scattering angle and 30, 60, and 100 eV incident electrons[43,44] are consistent with the photoabsorption results in Fig. 1. Figure 2 shows these electron energy-loss spectra, which cover the energy-loss range from 4 to 14 eV. Taken at forward scattering angles of 3°–10°, these spectra exhibit little variation with incident electron energy. They show distinct structure below the first ionization threshold energy at ~10.4 eV (see Table 5) with peaks at 4.7, 7.2, 8.1, 9.0, and 9.8 eV. The structure at 7.2 eV in the electron-energy-loss spectrum is consistent with that in the $\sigma_{pa,t}(\lambda)$ around 170 nm.

Photoionization, photodissociation, and electron-impact studies have provided values of the ionization threshold en-

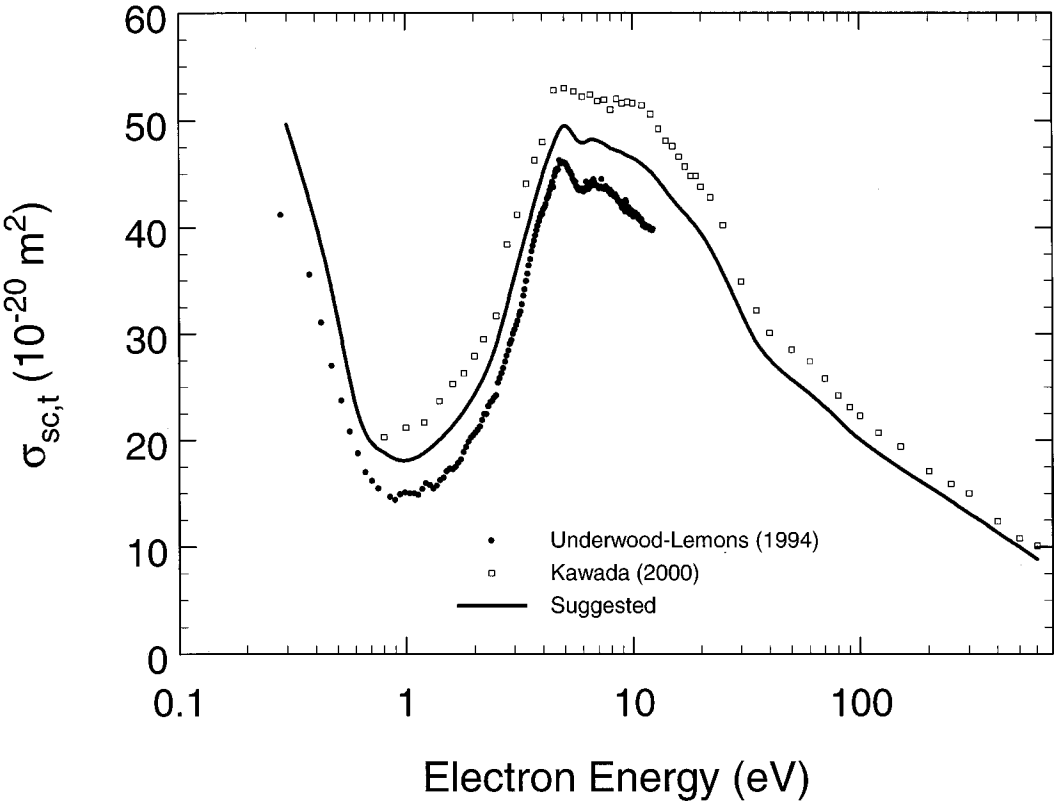

FIG. 3. Total electron scattering cross section as a function of electron energy, $\sigma_{sc,t}(\varepsilon)$, for CF_3I: (●) Ref. 40; (□) Ref. 60; (—) suggested.

ergies for the formation of CF_3I^+ and the various positive-ion fragments. These are listed in Table 5. It should be noted that some of the values listed for ionization to CF_3I^+ do not distinguish between the two ground states, $X^2E_{3/2}$ and $X^2E_{1/2}$, of CF_3I^+ which are separated by ~ 0.6 eV.

3. Total Electron Scattering Cross Section, $\sigma_{sc,t}(\varepsilon)$

Underwood-Lemons *et al.*[40] measured the total electron scattering cross section of CF_3I from ~ 0.5 to 12 eV, and Fig. 3 shows their data. The rise in the cross section below ~ 1 eV was attributed to the existence of a resonance of a_1 (C–Iσ^*) symmetry near zero energy, and the peak near 4.9 eV was tentatively ascribed to two negative-ion resonances of a_1 (C–Fσ^*) and e (C–Iπ^*) symmetries. Electron attachment studies[38] are consistent with the positions and assignments of these resonances, although Oster *et al.*[36] attributed the broad dissociative electron attachment resonance they observed near 4 eV to a temporary negative-ion state resulting from a two-particle (core excited) resonance associated with occupation of the LUMO of the neutral molecule. Kawada *et al.*[60] have also measured the total electron scattering cross section for CF_3I, in the energy range 0.8–600 eV. These data are also presented in Fig. 3, and although they fall systematically higher than the data of Underwood-Lemons *et al.*, the general shapes are in overall agreement.

We have derived our suggested data for $\sigma_{sc,t}(\varepsilon)$ for CF_3I by fitting a curve to the average of the two available data sets between 1 and 11 eV. The suggested data are then extended to higher and lower energies by normalizing the low energy data of Underwood-Lemons *et al.* to the average at 1 eV, and normalizing the high energy data of Kawada *et al.* to the average at 11 eV. These data are shown by the solid line in Fig. 3, and are presented in Table 6.

4. Differential Elastic Electron Scattering Cross Sections, $\sigma_{e,diff}$

Differential elastic electron scattering cross sections, $\sigma_{e,diff}$, have been measured by Kitajima *et al.*[43,44] for a number of electron energies between 1.5 and 60 eV over a scattering-angle range of 20°–130° in a crossed-beam experiment. The results of these measurements are shown in Fig. 4 and are listed in Table 7. Kitajima *et al.* indicated that the increases in the $\sigma_{e,diff}$ at low electron energies and small scattering angles result from electron-dipole scattering due to the permanent electric dipole moment of CF_3I. It was also noted by Okamoto *et al.*[42] that the largest contribution to the elastic differential scattering cross section comes predominantly from the I atom.

TABLE 6. Suggested values for the total electron scattering cross section, $\sigma_{sc,t}(\varepsilon)$, of the CF_3I molecule

Electron energy (eV)	$\sigma_{sc,t}(\varepsilon)$ (10^{-20} m^2)	Electron energy (eV)	$\sigma_{sc,t}(\varepsilon)$ (10^{-20} m^2)
0.30	49.6	9.5	46.7
0.40	40.5	10.0	46.5
0.50	31.5	11	45.9
0.60	23.3	12	45.2
0.70	19.8	15	42.6
0.80	18.8	20	39.5
0.90	18.2	25	35.7
1.00	18.1	30	32.0
1.25	19.1	35	29.2
1.50	20.7	40	27.6
1.75	22.4	45	26.5
2.0	24.3	50	25.7
2.5	29.0	60	24.4
3.0	35.3	70	23.1
3.5	40.5	80	21.9
4.0	44.9	90	20.9
4.5	47.9	100	20.0
5.0	49.5	150	17.3
5.5	48.6	200	15.6
6.0	47.9	250	14.3
6.5	48.2	300	13.1
7.0	48.1	350	12.2
7.5	47.8	400	11.3
8.0	47.4	450	10.6
8.5	47.2	500	9.97
9.0	47.0	600	8.82

5. Momentum Transfer Cross Section, $\sigma_m(\varepsilon)$

To our knowledge no measurements have been reported of the momentum transfer cross section, $\sigma_m(\varepsilon)$, for the CF_3I molecule. However, since CF_3I is polar, an estimate of its momentum transfer cross section at low electron energies (below ~ 0.5 eV) can be made using the Altshuler[61] formula

$$\sigma_m(v)(\mathrm{cm}^2) = (1.72D^2)/v^2, \tag{1}$$

where D is the dipole moment of the CF_3I molecule in debye units, v is the electron velocity, and the cross section $\sigma_m(v)$ is expressed in units of cm^2. Experimental studies on other polar molecules have shown[62,63] that at low electron energies ($\lesssim 0.5$ eV) the total electron scattering cross section is within about a factor of 2 of the values of $\sigma_m(v)$ predicted by Eq. (1) [see also similar findings for CHF_3 in Ref. 12]. Taking the average dipole moment (0.96 D) given by McClellan,[19] Eq. (1) predicts the $\sigma_m(\varepsilon)$ values listed in Table 8.

6. Differential Vibrational Excitation Cross Section, $\sigma_{vib,diff}(\varepsilon)$

Okamoto *et al.*[42] and Kitajima *et al.*[43] used a crossed-beam apparatus to measure the differential vibrational excitation cross section, $\sigma_{vib,diff}(\varepsilon)$, of CF_3I for an electron-energy loss of 0.14 eV (due mainly to excitation of the CF_3 stretching modes) and a scattering angle of 60°, as a function of the incident electron energy from 1.5 to 17 eV. This cross section is shown in Fig. 5. The enhancements near 5.5 and 8 eV were attributed[42,43] to negative ion resonances. The sharp increase in the cross section with decreasing electron energy below ~ 2 eV is attributed to another resonance at energies below 1 eV, in agreement with the electron attachment data (Table 3).

7. Electron-Impact Ionization

7.1. Partial Ionization Cross Sections, $\sigma_{i,partial}(\varepsilon)$

There have been two unpublished measurements of the partial ionization cross sections, $\sigma_{i,partial}(\varepsilon)$, of CF_3I, both employing Fourier transform mass spectrometry. The first made by Riehl[58] in 1992, and the second by Jiao *et al.*[64] in 1999. The measurements of Riehl[58] were calibrated using the data of Wetzel *et al.*[65] for Xe at an energy of 25 eV and have a quoted uncertainty in excess of $\pm 30\%$. The measurements of Jiao *et al.*[64] were normalized to the data of Wetzel *et al.*[65] for Ar at 50 eV and have an uncertainty of about $\pm 22\%$ (the uncertainty in the energy scale of both studies is about ± 0.5 eV). Since both of these sets of measurements were made at the same laboratory, and since the more recent data have a smaller uncertainty, we show in Fig. 6 only the more recent measurements for electron-impact production of CF_3I^+, CF_2I^+, CF_3^+, CF_2^+, CF^+, and I^+. Over the energy range covered by these measurements ($\leqslant 70$ eV), CF_3I^+ is the most abundant positive ion followed by I^+, CF_3^+, and CF_2I^+. The cross sections for CF_2^+ and CF^+ are about a factor of ten smaller. Riehl[58] estimated the cross section for the production of F^+ to be less than 2×10^{-18} cm^2 for electron energies below 50 eV.

In the absence of published data on the $\sigma_{i,partial}(\varepsilon)$ of CF_3I, we list in Table 9 the measurements of Jiao *et al.*[64] as our presently suggested values for the partial ionization cross sections for this molecule.

The relative abundances of the various positive ions formed by electron impact on CF_3I as measured by Jiao *et al.*[64] at 70 eV, differ considerably from the 70 eV ''cracking pattern'' of the CF_3I molecule reported in Heller and Milne.[66] The ratio of the Jiao *et al.* partial ionization cross sections at 70 eV for the ions CF_3I^+:I^+:CF_3^+:CF_2^+:CF^+ is 100:90.3:34.7:5.2:8.5, while Heller and Milne list, respectively, 100:95.6:77.4:7.3:11.6. The higher relative intensities of the lower mass ions measured by Heller and Milne, as compared to the measurements of Jiao *et al.*, indicate possible discrimination against high-mass ions common to quadrupole mass spectrometers. (For ion-molecule reactions in-

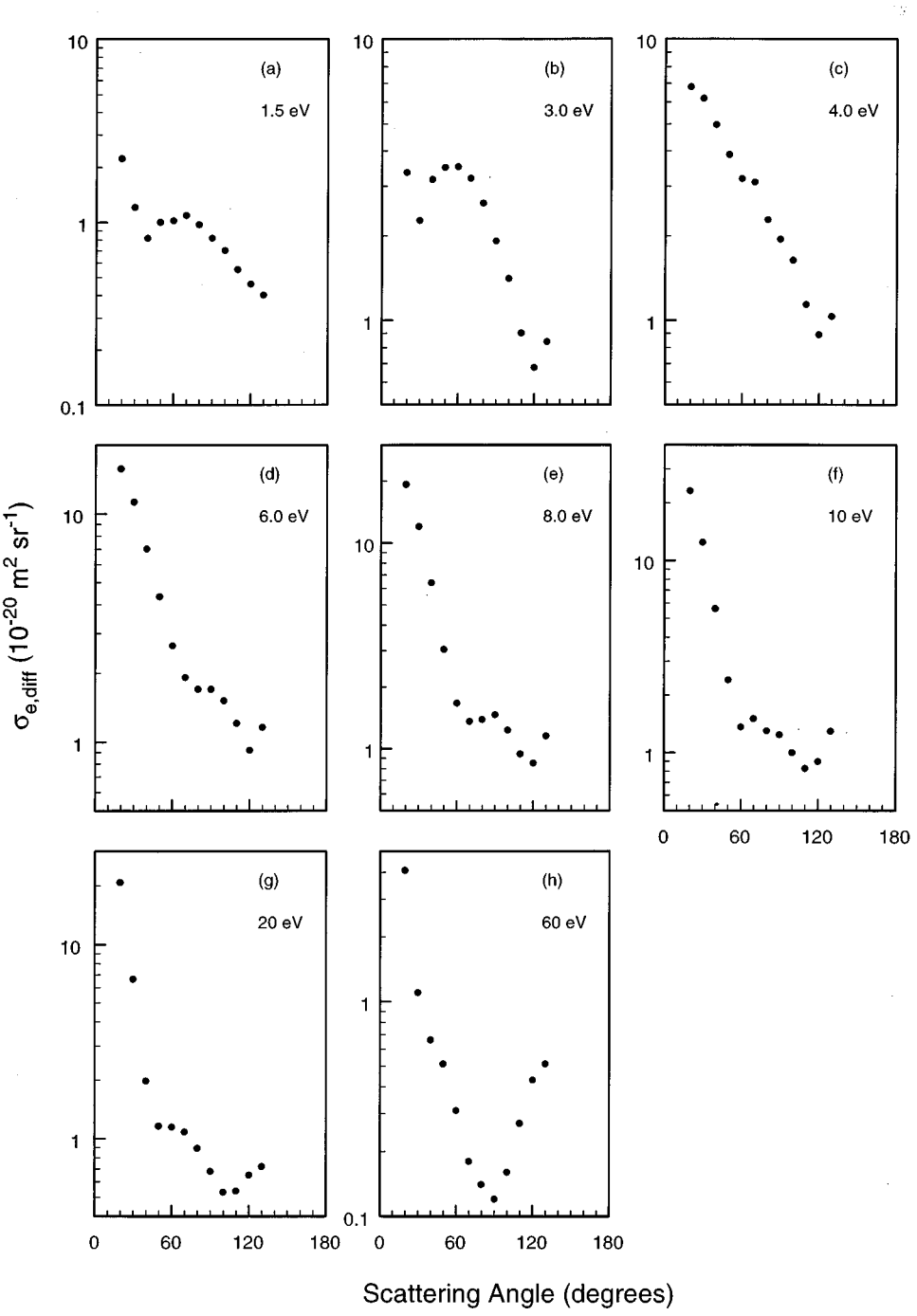

FIG. 4. Differential elastic electron scattering cross sections, $\sigma_{e,diff}$, for CF_3I at a number of n cident electron energies [data of Kitajima *et al.* from Ref. 43, as provided to the authors by Professor H. Tanaka (Ref. 44)].

volving I^+ and CF_3^+ with CF_3I see Berman *et al.*,[54] and for formation of CF_3I^+ in photoinduced charge transfer at surfaces see Sun *et al.*[67]).

7.2. Total Ionization Cross Section, $\sigma_{i,t}(\varepsilon)$

The total ionization cross section, $\sigma_{i,t}(\varepsilon)$, of CF_3I obtained by summing the partial ionization cross sections of Jiao *et al.*[64] is shown in Fig. 7. The error bar shown in the figure indicates the $\pm 22\%$ uncertainty of the partial ionization cross sections. Also plotted in Fig. 7 is the value $[(10.9 \pm 0.48) \times 10^{-16}\,\mathrm{cm}^2]$ of $\sigma_{i,t}(\varepsilon)$ of CF_3I measured by Beran and Kevan[68] for 70 eV incident electrons. The values agree within the combined uncertainty of the two measurements. The data of Jiao *et al.* are listed in Table 10 as our presently suggested values for the $\sigma_{i,t}(\varepsilon)$ of CF_3I.

To our knowledge no measurements of the electron-impact ionization coefficient have been made for this molecule.

TABLE 7. Differential elastic electron scattering cross sections, $\sigma_{e,diff}$, of CF_3I (in units of $10^{-20}\,m^2\,sr^{-1}$) for a number of incident electron energies (data of Kitajima *et al.* from Refs. 43 and 44)

	Electron energy (eV)							
Angle	1.5	3	4	6	8	10	20	60
20°	2.22	3.35	6.79	15.7	19.3	23.0	20.8	4.06
30°	1.21	2.27	6.16	11.2	12.0	12.4	6.62	1.10
40°	0.82	3.16	4.96	7.01	6.40	5.62	1.98	0.66
50°	1.00	3.49	3.88	4.33	3.03	2.39	1.16	0.51
60°	1.02	3.52	3.18	2.65	1.67	1.36	1.15	0.31
70°	1.09	3.20	3.10	1.92	1.36	1.50	1.08	0.18
80°	0.97	2.61	2.28	1.70	1.39	1.30	0.89	0.14
90°	0.82	1.91	1.94	1.70	1.46	1.24	0.68	0.12
100°	0.70	1.41	1.63	1.52	1.23	1.00	0.53	0.16
110°	0.55	0.90	1.14	1.21	0.94	0.82	0.54	0.27
120°	0.46	0.68	0.89	0.92	0.85	0.90	0.65	0.43
130°	0.40	0.84	1.03	1.16	1.15	1.29	0.72	0.51

8. Electron Attachment

8.1. Relative Cross Sections for the Production of the Fragment Negative Ions I^-, F^-, CF_3^-, and FI^- by Dissociative Electron Attachment to CF_3I

There have been a number of studies of electron attachment to CF_3I. These include electron-beam measurements of the relative cross sections for the formation of the various fragment negative ions,[27,34–37,41,69] electron-beam measurements of the total electron attachment cross section,[38,39] electron-swarm measurements of the thermal-electron attachment rate constant,[70–73] very-low-energy electron-beam total electron attachment cross-section measurements,[74] and measurements of the rate constant of bound-electron attachment at thermal and subthermal electron energies.[75,76]

Based on the results of these studies, electron attachment to CF_3I produces I^-, F^-, CF_3^-, and FI^- negative ions, mainly *via* two dissociating negative-ion states, one at ~ 0.0 eV and another near 3.8 eV. This is seen from the measurements of Oster *et al.*[36] shown in Fig. 8. The zero-energy process generates I^- *via* the reaction

$$e + CF_3I \rightarrow I^- + CF_3 \tag{2}$$

and is exothermic by $-(0.67 \pm 0.1)$eV.[36] The 3.8 eV process generates F^-, CF_3^-, and FI^-. The fragment anions F^- and CF_3^- are generated via the reactions

$$e + CF_3I \rightarrow F^- + CF_2I, \tag{3a}$$

$$e + CF_3I \rightarrow CF_3^- + I. \tag{3b}$$

Reactions (3a) and (3b) are endothermic, respectively, by $(\sim 1.5 \pm 0.3)$ eV,[36] and by (0.7 ± 0.3) eV.[36] According to Oster *et al.*,[36] the weak F^- signal near 0.0 eV does not arise from the direct dissociative electron attachment process, Eq. (3a), but rather from an ion–molecule reaction of the form $I^- + CF_3I \rightarrow F^- + CF_2I_2$.

The formation of the FI^- ion has an ''appearance energy'' of (2.2 ± 0.2) eV and requires a multiple dissociation process.[35] Interestingly, the complementary reaction to Eq. (3b), that is, the production of $I^- + CF_3$ was not observed from the 3.8 eV negative ion state.[35,36]

Reactions (2) and (3b) result from breaking the C–I bond as a result of localization of the extra electron into a molecular orbital with antibonding σ^*_{C-I} character. This is supported by theoretical calculations[40] and also by the fact that, in the formation of CF_3^- at threshold, the total excess energy of the transient anion appears as kinetic energy of the dissociation products.[35] This is also consistent with photoabsorption and photodissociation studies. For instance, Suh *et al.*[77] found

TABLE 8. Calculated values of $\sigma_m(\varepsilon)$ for CF_3I determined via Eq. (1) and using for the dipole moment of CF_3I the value of 0.96 D

Electron energy (eV)	$\sigma_m(\varepsilon)$ $(10^{-20}\,m^2)$
0.005	902
0.01	451
0.05	90.2
0.10	45.1
0.50	9.0

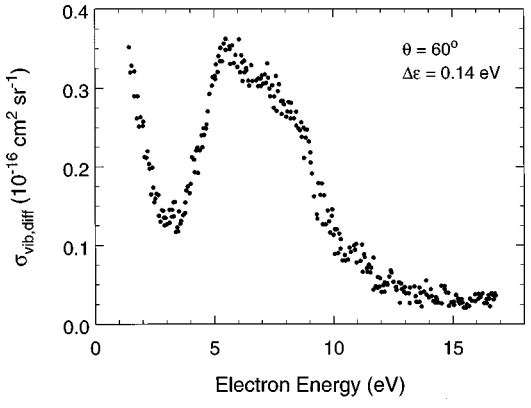

FIG. 5. Differential vibrational excitation cross section as a function of the incident electron energy, $\sigma_{vib,diff}(\varepsilon)$, for CF_3I [data of Kitajima *et al.* from Ref. 43, as provided to the authors by Professor H. Tanaka (Ref. 44)]. The measurements are for a scattering angle of 60° and an electron-energy loss of 0.14 eV.

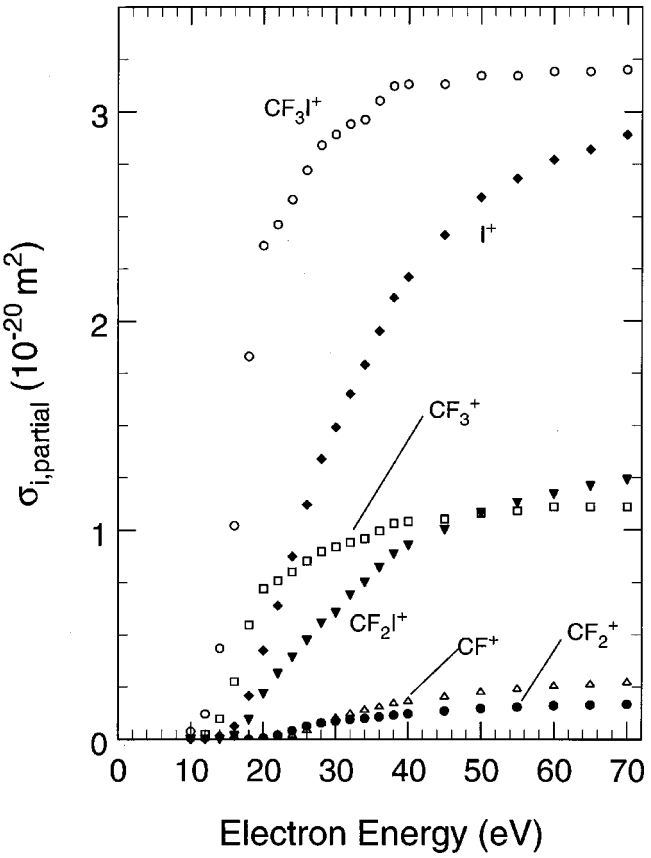

FIG. 6. Partial ionization cross sections, $\sigma_{i,partial}(\varepsilon)$, for CF_3I (data of Jiao *et al.* from Ref. 64).

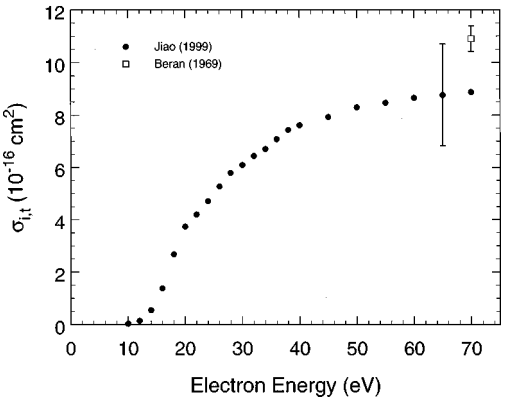

FIG. 7. Total ionization cross section, $\sigma_{i,t}(\varepsilon)$, for CF_3I: (●) Ref. 64; (□) Ref. 68.

that in the photodissociation of CF_3I at 266 nm (4.66 eV), 85% of the available energy is partitioned into translational energy.

In addition to the dissociative electron attachment processes, Eqs. (2) and (3), F^- and CF_3^- ions have been observed, respectively, at energies above 12.3 and 11.8 eV,[35,36] and their production at these energies has been attributed to the nonresonant ion-pair-formation processes

$$e + CF_3I \rightarrow CF_3I^* + e \tag{4a}$$

$$\hookrightarrow F^- + CF_2I^+ \tag{4b}$$

$$\hookrightarrow CF_3^- + I^+. \tag{4c}$$

TABLE 9. Suggested values for the partial ionization cross sections, $\sigma_{i,partial}(\varepsilon)$, of CF_3I (data of Jiao *et al.* from Ref. 64)

Electron energy (eV)	$\sigma_{i,partial}(\varepsilon)$ (10^{-20} m^2)					
	CF^+	CF_2^+	CF_3^+	I^+	CF_2I^+	CF_3I^+
10						0.0389
12			0.0246			0.121
14			0.0978	0.0180		0.435
16			0.277	0.0629	0.0161	1.02
18			0.547	0.208	0.0929	1.83
20		0.0064	0.720	0.425	0.219	2.36
22	0.0048	0.0193	0.759	0.640	0.313	2.46
24	0.0176	0.0418	0.800	0.874	0.392	2.58
26	0.0418	0.0626	0.852	1.12	0.473	2.72
28	0.0755	0.0780	0.896	1.34	0.555	2.84
30	0.101	0.0864	0.919	1.49	0.604	2.89
32	0.121	0.0946	0.940	1.65	0.690	2.94
34	0.140	0.100	0.958	1.79	0.750	2.96
36	0.155	0.107	0.995	1.95	0.820	3.05
38	0.171	0.115	1.03	2.11	0.885	3.12
40	0.181	0.122	1.04	2.21	0.925	3.13
45	0.202	0.135	1.05	2.41	1.00	3.13
50	0.225	0.147	1.08	2.59	1.08	3.17
55	0.240	0.154	1.09	2.68	1.13	3.17
60	0.253	0.160	1.11	2.77	1.17	3.19
65	0.261	0.164	1.11	2.82	1.21	3.19
70	0.271	0.167	1.11	2.89	1.24	3.20

TABLE 10. Suggested values for the total ionization cross section, $\sigma_{i,t}(\varepsilon)$, of CF_3I (data of Jiao *et al.* from Ref. 64)

Electron energy (eV)	$\sigma_{i,t}(\varepsilon)$ $(10^{-20}\,m^2)$	Electron energy (eV)	$\sigma_{i,t}(\varepsilon)$ $(10^{-20}\,m^2)$
10	0.039	32	6.44
12	0.146	34	6.70
14	0.551	36	7.08
16	1.38	38	7.43
18	2.68	40	7.61
20	3.73	45	7.93
22	4.20	50	8.29
24	4.71	55	8.46
26	5.27	60	8.65
28	5.78	65	8.76
30	6.09	70	8.88

The CF_3I^- parent negative ion has not been observed in any of the gas-phase electron attachment studies, however, it is known to be formed in charge-transfer reactions involving K, Na, and Cs atoms[24–26] and by electron attachment to CF_3I clusters.[36] Interestingly, in a study of the desorption of CF_3^- following the interaction of low-energy (0–10 eV) electrons with a CF_3I film,[37] the desorption cross section was found to be more than two orders of magnitude greater than the corresponding gas-phase dissociative electron attachment cross section.

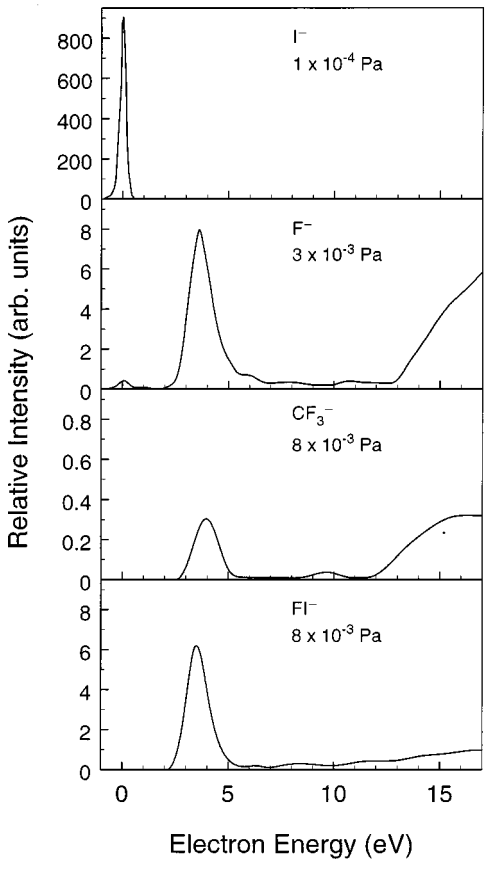

FIG. 8. Relative cross sections for the formation of I^-, F^-, CF_3^-, and FI^- by dissociative electron attachment to CF_3I for $T=300$ K (data of Oster *et al.* from Ref. 36). Note the pressures in comparing the magnitudes of the relative cross sections of the various negative ions. The work of Oster *et al.* indicates possible production of I^- at higher energies than the zero-energy peak.

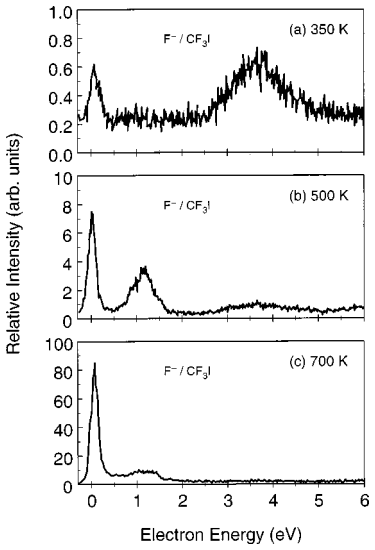

FIG. 9. Variation with gas temperature of the relative cross section for the formation of F^- by dissociative electron attachment to CF_3I (data of Hahndorf and Illenberger from Ref. 41).

8.2. Effect of Temperature on the Production of F^- by Dissociative Electron Attachment to CF_3I

Figure 9 shows the relative cross section for the formation of F^- by dissociative electron attachment to CF_3I at three temperatures (350, 500, and 700 K) as reported by Hahndorf and Illenberger.[41] The weak F^- signal at ~ 0.0 eV in the room temperature measurements (Fig. 8) increases substantially with increasing temperature above ambient, however, even at 700 K the relative cross section for the formation of F^- is small compared with that for the formation of I^- at this energy. Additionally, in view of the magnitude and energy dependence of the cross section for I^- production, it is not expected that the I^- signal will exhibit a significant temperature dependence.[78] Hence, for temperatures in this range, the total electron attachment cross section as measured by Underwood-Lemons *et al.*,[38] and the total thermal-electron attachment-rate constant as measured by various groups (see Table 13 in Sec. 8.5) should not be considerably affected by the gas temperature, as is indeed the case (see Fig. 10 in Sec. 8.3). Moreover, the data in Fig. 9 indicate that the production of F^- from CF_3I has another maximum between 1 and 2 eV. This is consistent with earlier observations of a negative-ion peak around 1 eV by Marriott and Craggs[27] and by Buchel'nikova[39] (see Table 3).

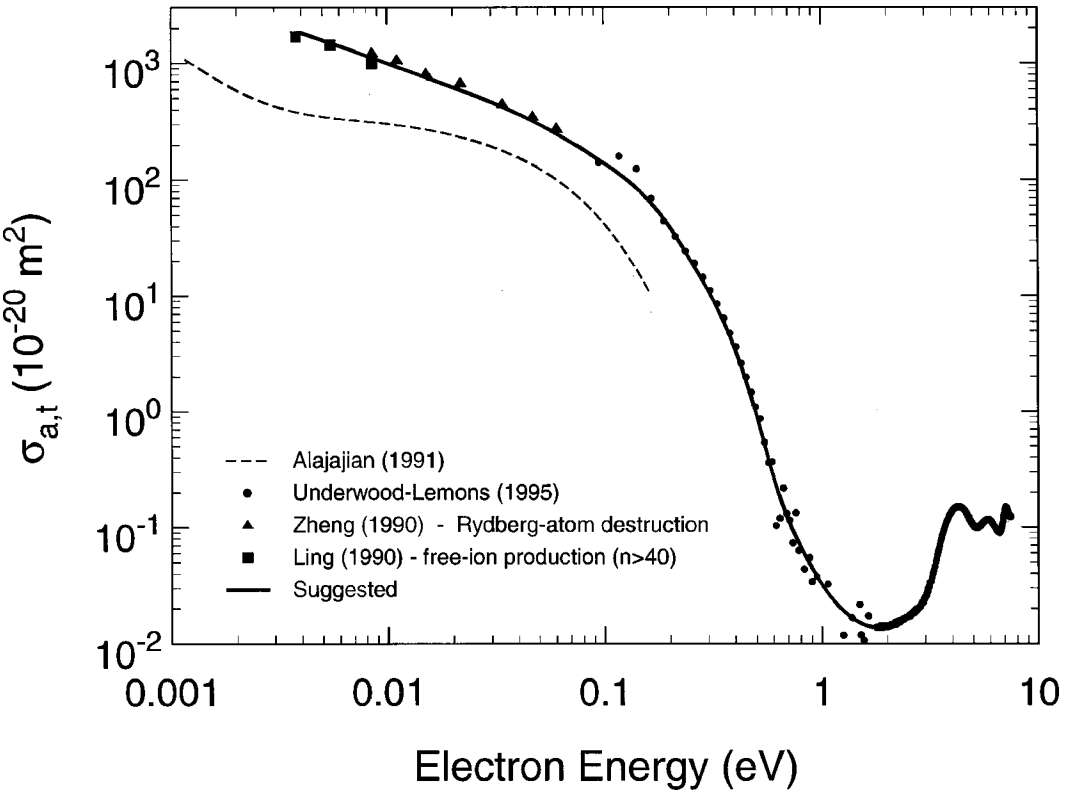

FIG. 10. Total electron attachment cross section as a function of electron energy, $\sigma_{a,t}(\varepsilon)$, for CF_3I. *Free-electron attachment*: (- - -) Ref. 74; (●) Ref. 38. *Bound-electron attachment*: (▲) Rydberg-atom destruction data from Ref. 75; (■) free-ion production data ($n>40$) from Ref. 76. (—) Suggested values.

8.3. Total Electron Attachment Cross Section as a Function of Electron Energy, $\sigma_{a,t}(\varepsilon)$

The total electron attachment cross section, $\sigma_{a,t}(\varepsilon)$, of CF_3I has been measured by Underwood-Lemons[38,79] for electron energies $\leqslant 7.5$ eV under single-collision conditions and temperatures of 393 and 563 K. Figure 10 shows the data from the measurements made at 393 K. No significant temperature effects were observed. The peak energy and symmetry assignment of the negative-ion resonances observed in a total electron-scattering cross section study[40] are given in Table 3. The steep rise of the cross section toward zero energy is attributed to electron capture into the LUMO of CF_3I with a_1 symmetry and σ^*(C–I) bonding character. The fragment ion is thus I^- [Reaction (2)]. In contrast, the fragment negative-ion peak near 4.5 eV is associated with the next higher unoccupied orbital a_1 (C–Fσ^*). The primary ion associated with this resonance is thus F^- [Reaction (3a)].

Also plotted in Fig. 10 are the total electron attachment cross sections of Alajajian *et al.*[74] determined using the Kr photoionization method for the production of monoenergetic low-energy electrons. The relative cross section values obtained by this method were put on an absolute scale by normalization to the thermal ($T=300$ K) electron attachment-rate-constant value of Shimamori and Nakatani[70] (see Table 13 in Sec. 8.5).

In addition to the data of Alajajian *et al.*,[74] two other measurements of $\sigma_{a,t}(\varepsilon)$ for CF_3I in the low-energy range have been plotted in Fig. 10. The first is derived from the rate constant, $k_{d,Ryd}(n)$, for the destruction of the Rydberg atoms $K^*(nd)$ in collision with CF_3I.[75] The second is derived from the rate for negative-ion formation, $k_{d,be}(n)$, in collisions of $K^*(nd)$ with CF_3I.[76] In both cases n is the principal quantum number of the Rydberg electron. The rate $k_{d,be}(n)$ refers to the reaction

$$K^*(nd)+CF_3I \rightarrow K^+ + CF_3I^{-*} \rightarrow K^+ + CF_3 + I^-, \quad (5)$$

and is less than or equal to $k_{d,Ryd}(n)$ since the probability of escape of I^- can be less than one. As can be seen from Fig. 11, the difference between $k_{d,Ryd}(n)$ and $k_{a,be}(n)$ depends on the value of n. As n becomes small, postattachment electrostatic attraction between the product ions (I^- and K^+) becomes important causing larger differences between the two rate constants.

The bound-electron attachment rate constants, $k_{d,Ryd}(n)$ (data of Ref. 75) and $k_{a,be}(n)$ (data of Ref. 76), were converted to functions of the electron energy using the relationship $\varepsilon = R/v^2$, where R is the Rydberg constant (13.6 eV). These values were then used to determine the bound-electron attachment cross section, $\sigma_{a,be}(\varepsilon)$ (and similarly $\sigma_{d,Ryd}(\varepsilon)$), from

$$\sigma_{a,be}(v) = k_{a,be}(n)/v_{rms}, \quad (6)$$

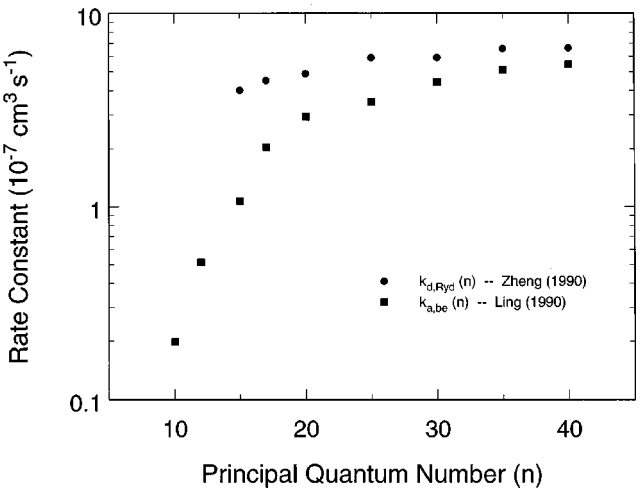

FIG. 11. Rate constants, $k_{d,Ryd}(n)$, for Rydberg-atom destruction (●, Ref. 75), and, $k_{a,be}(n)$, for negative-ion production (■, Ref. 76) in collisions of $K^*(nd)$ with CF_3I as a function of n (see text).

where v_{rms} is the root-mean-square velocity of the Rydberg electron. All values of $\sigma_{d,Ryd}(\varepsilon)$ determined this way are shown in Fig. 10, however, for $\sigma_{a,be}(\varepsilon)$ we have plotted only the data for $n \geqslant 40$ since a number of studies[18,80–82] have indicated that Eq. (6) is expected to be valid only for large values of $n(>30)$. Figure 10 shows that the low-energy bound-electron attachment data agree well with the higher-energy electron-beam measurements of Underwood-Lemons *et al.*[38] However, both sets of data disagree with the data of Alajajian *et al.*,[74] that were obtained by normalizing to the swarm attachment rate constant. This may indicate a difference in the magnitude of the electron attachment rate constant near thermal energies as determined by swarm methods and by techniques employing bound electron capture processes (see discussion in next section).

The data in Fig. 10 show that at thermal energy ($\varepsilon \simeq 0.038$ eV, $T = 300$ K), the total electron attachment cross section exceeds 10^{-14} cm^2. This value is more than two orders of magnitude greater than the value of 7.8×10^{-17} cm^2 of the cross section measured by Buchel'nikova[39] at ~ 0.0 eV, which is not shown in Fig. 10.

The data of Underwood-Lemons *et al.*,[38] Zheng *et al.*,[75] and Ling *et al.*[76] are in agreement, and the solid line in Fig. 10 is a fit to these three sets of data. Values from this curve are listed in Table 11 as our suggested data for the $\sigma_{a,t}(\varepsilon)$ of CF_3I.

TABLE 11. Suggested values for the total electron attachment cross section, $\sigma_{a,t}(\varepsilon)$, of CF_3I

Electron energy (eV)	$\sigma_{a,t}(\varepsilon)$ (10^{-20} m^2)	Electron energy (eV)	$\sigma_{a,t}(\varepsilon)$ (10^{-20} m^2)
0.004	1820	0.70	0.114
0.005	1575	0.80	0.067
0.006	1399	0.90	0.044
0.007	1265	1.00	0.032
0.008	1157	1.50	0.015
0.009	1070	2.00	0.014
0.010	997	2.50	0.017
0.015	757	3.00	0.026
0.020	623	3.50	0.070
0.025	532	4.00	0.138
0.030	464	4.25	0.148
0.040	369	4.50	0.140
0.050	302	4.75	0.122
0.060	251	5.00	0.104
0.070	212	5.25	0.100
0.080	183	5.50	0.107
0.090	158	5.75	0.115
0.10	139	6.00	0.112
0.15	76.1	6.25	0.102
0.20	39.4	6.50	0.092
0.25	19.9	6.75	0.098
0.30	11.1	7.00	0.135
0.40	3.38	7.25	0.134
0.50	0.930	7.50	0.118
0.60	0.266		

8.4. Total Electron Attachment Rate Constant as a Function of the Mean Electron Energy, $k_{a,t}(\langle\varepsilon\rangle)$

The measurements of $k_{a,t}(\langle\varepsilon\rangle)$ by Shimamori *et al.*[71] and Sunagawa and Shimamori[73] are shown in Fig. 12. A pulse-radiolysis microwave-cavity method was employed with provisions for electron heating above thermal energies and an indirect method of determining the mean electron energy (see Ref. 71 for details). Also shown in the figure are the $k_{a,t}(\langle\varepsilon\rangle)$ measurements of Alajajian *et al.*[74] They used the Kr photoionization technique for the production of monoenergetic low-energy electrons and the room temperature ($T = 300$ K) thermal-electron attachment-rate constant, $(k_{a,t})_{th}$, of Shimamori and Nakatani[70] (1.7×10^{-7} cm^3 s^{-1}, see Table 13 in Sec. 8.5) for normalization of their relative data. The average of the four ''room temperature'' values of $(k_{a,t})_{th}$ (Table 13, Sec. 8.5) is 1.9×10^{-7} cm^3 s^{-1}, and this value is also plotted in Fig. 12. Additionally, we have plotted in Fig. 12 the values of $k_{d,Ryd}(n)$ measured by Zheng *et al.*[75] and the values of $k_{a,be}(n)$ for $n>40$ measured by Ling *et al.*[76]

The bound-electron attachment measurements indicate higher values of the electron attachment rate constant than the electron swarm measurements. At thermal ($T \approx 300$ K) energies the electron swarm data are lower by about a factor of 2. This difference is not understood, and complicates the determination of suggested values for the $k_{a,t}(\langle\varepsilon\rangle)$ of this molecule. Because all four independent measurements of the thermal ($T \approx 300$ K) value of $k_{a,t}(\langle\varepsilon\rangle)$ are in essential agreement (they are within the quoted or expected uncertainties), we opted to fit only the electron swarm data in Fig. 12 in an effort to determine suggested values for $k_{a,t}(\langle\varepsilon\rangle)$. Our fit to the swarm data is shown by the solid line, and values from this line are listed in Table 12 as our suggested data for $k_{a,t}(\langle\varepsilon\rangle)$ of CF_3I.

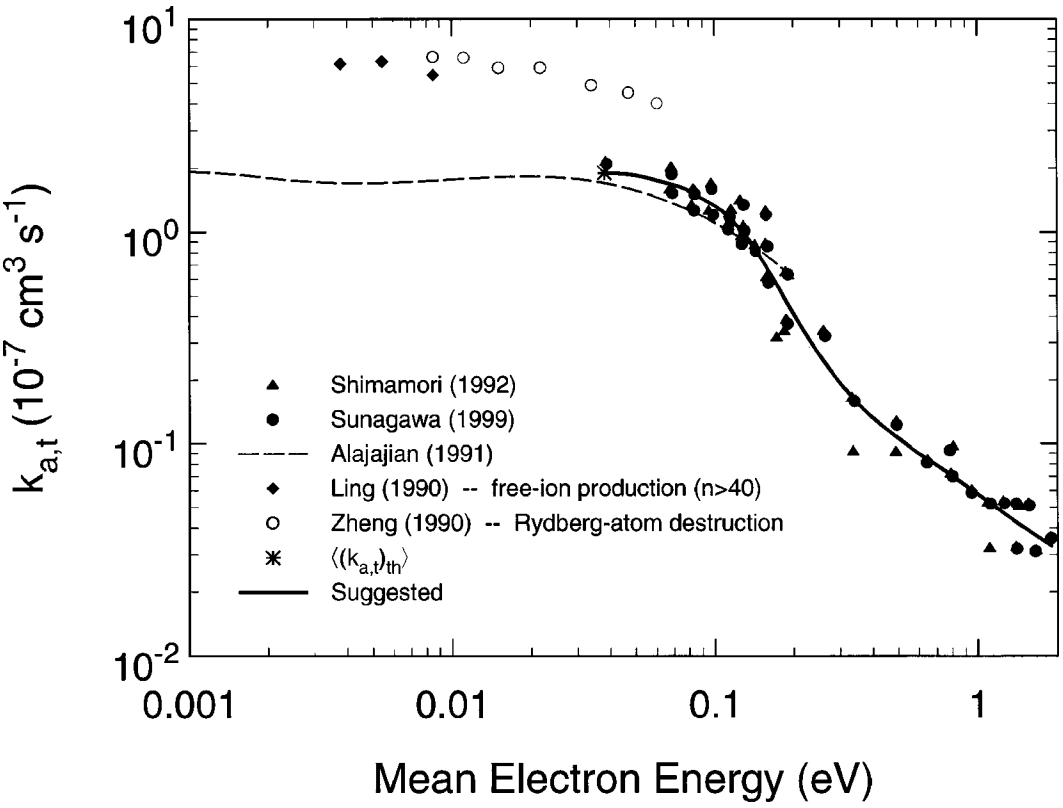

FIG. 12. Total electron attachment rate constant as a function of the mean electron energy, $k_{a,t}(\langle\varepsilon\rangle)$, for CF_3I. *Swarm data*: (▲) Ref. 71; (●) Ref. 73. *Low-energy electron beam data*: (- - -) Ref. 74. *Bound-electron attachment data*: (○) Rydberg-atom destruction data from Ref. 75; (♦) free-ion production data ($n>40$) from Ref. 76. (*) Average thermal value (1.9×10^{-7} cm^3 s^{-1}) of the room temperature swarm measurements (see text). (—), Suggested values for $k_{a,t}(\langle\varepsilon\rangle)$.

8.5. Thermal Electron Attachment Rate Constant, $(k_{a,t})_{th}$

The available data on the thermal value of the electron attachment rate constant, $(k_{a,t})_{th}$, are listed in Table 13. The room-temperature values of $(k_{a,t})_{th}$ are within the combined quoted uncertainties. Their average is 1.9×10^{-7} cm^3 s^{-1}.

Interestingly, the measurements of $(k_{a,t})_{th}$ in Fig. 13 show a small increase with increasing T from 250 to 500 K and a decline beyond 600 K. This is consistent with other observations[78] involving strong dissociative electron attachment processes peaking at ~0 eV when the potential energy curve of the dissociating negative ion state crosses that of the ground state of the neutral molecule in such a way that population of vibrational levels higher than the $\nu=0$ of the neutral molecule results in the initial state of the neutral molecule lying above the dissociating negative ion state.

TABLE 12. Suggested values for the total electron attachment rate constant, $k_{a,t}(\langle\varepsilon\rangle)$, of CF_3I

Mean electron energy (eV)	$k_{a,t}(\langle\varepsilon\rangle)$ (10^{-7} cm^3 s^{-1})	Mean electron energy (eV)	$k_{a,t}(\langle\varepsilon\rangle)$ (10^{-7} cm^3 s^{-1})
0.038	1.90	0.4	0.13
0.05	1.85	0.5	0.11
0.06	1.75	0.6	0.089
0.07	1.66	0.7	0.079
0.08	1.56	0.8	0.070
0.09	1.43	0.9	0.063
0.10	1.33	1.0	0.058
0.15	0.75	1.5	0.040
0.20	0.41	1.9	0.033
0.30	0.19		

TABLE 13. Thermal values, $(k_{a,t})_{th}$, of the total electron attachment rate constant of CF_3I

$(k_{a,t})_{th}$ (10^{-7} cm^3 s^{-1})	T (K)	Reference
1.5	250	70
1.7±0.2	~300	70
2.0	350	70
1.9±0.1	300	83
2.0±0.2	~300	71
2.2	293	72
2.4	615	72
2.2	777	72
1.5	1022[a]	72

[a]Data suspected for possible error due to possible thermal decomposition of the gas.

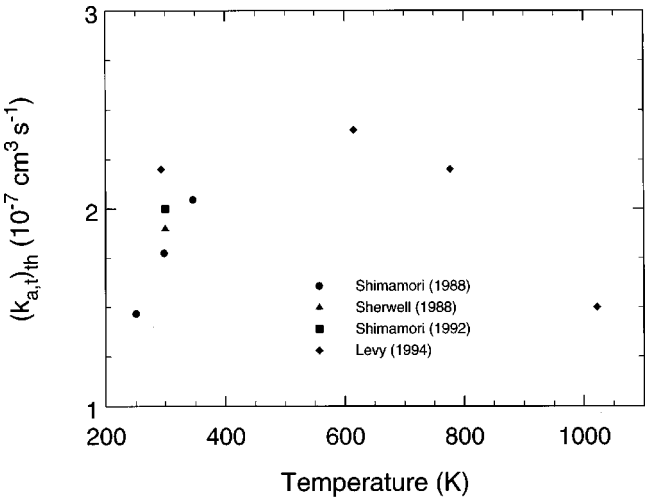

FIG. 13. Temperature dependence of the thermal electron attachment rate constant, $(k_{a,t})_{th}$, of CF_3I: (●) Ref. 70; (▲) Ref. 83; (■) Ref. 71; (◆) Ref. 72.

9. Optical Emission Under Electron Impact

Martínez *et al.*[84] performed an experimental study of the visible and ultraviolet emissions following pulsed electron-impact on CF_3I. For electron-impact energies of 100 eV, the spectra in the 200–600 nm region show a number of narrow lines superimposed on two broad bands centered at 300 and 470 nm. The emission bands were attributed[84] to the CF_3^* and IF* species and the atomic lines to the I_I^* and I_{II}^* fragments.

10. Summary of Cross Sections

The meager data on the electron scattering cross sections for CF_3I are summarized in Fig. 14. The suggested values for $\sigma_{sc,t}(\varepsilon)$ (Fig. 3; Table 6), $\sigma_{i,t}(\varepsilon)$ (Fig. 7; Table 10), and $\sigma_{a,t}(\varepsilon)$ (Fig. 10; Table 11) are shown by solid lines, and the calculated values of $\sigma_m(\varepsilon)$ (Table 8) are shown by a dashed line.

The values of $\sigma_{pa,t}(\lambda)$ (Table 4), $\sigma_{e,diff}$ (Table 7), and $\sigma_{i,partial}(\varepsilon)$ (Table 9) are also suggested but are not plotted in Fig. 14.

11. Data Needs

With the exception of the total electron scattering, electron-impact ionization, and electron attachment cross sections, measurements of the cross sections for all other electron collision processes are needed. Even the cross sections for total electron scattering, electron attachment, and electron-impact ionization need further investigation to confirm the limited data that are presently available and to extend the range of energies over which data are available.

No experimental data are available for the electron transport, ionization, and attachment coefficients of this molecule.

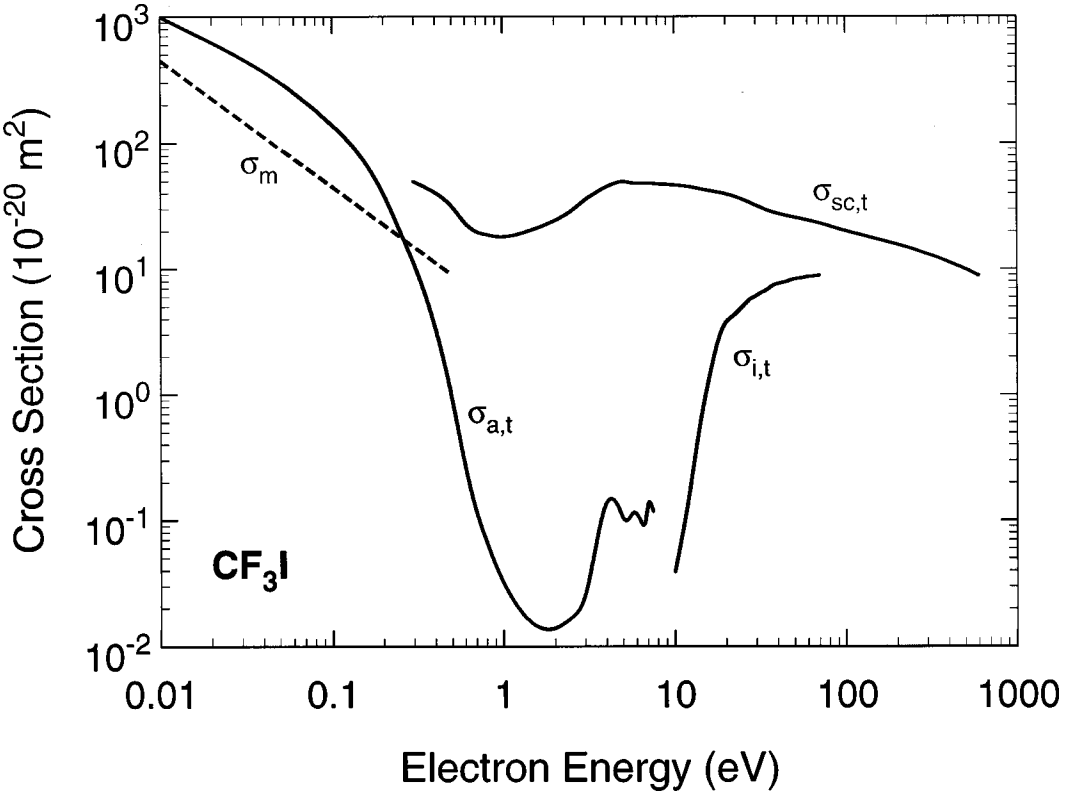

FIG. 14. Summary of suggested electron collision cross sections for CF_3I (see the text).

12. Acknowledgments

We thank Professor H. Tanaka (Sophia University) for providing us with his data on the differential electron scattering cross sections, Dr. C. Jiao (Wright Laboratory) for providing us with his measurements of the partial and total electron-impact ionization cross sections, and for bringing to our attention the earlier measurements by K. B. Riehl, Professor M. Kimura (Yamaguchi University) for providing us with a preprint of their paper on CF_3I, and Dr. P. Haaland (Mobium Enterprises) for providing parts of K. B. Riehl's dissertation.

13. References

[1] S. M. Karecki, L. C. Pruette, and L. R. Reif, Mater. Res. Soc. Symp. Proc. **447**, 67 (1997).
[2] S. M. Karecki, L. C. Pruette, and L. R. Reif, J. Vac. Sci. Technol. A **16**, 755 (1998).
[3] R. A. Levy, V. B. Zaitsev, K. Aryusook, C. Ravindranath, V. Sigal, A. Misra, S. Kesari, D. Rufin, J. Sees, and L. Hall, J. Mater. Res. **13**, 2643 (1998).
[4] F. Fracassi and R. d'Agostino, J. Vac. Sci. Technol. B **16**, 1867 (1998).
[5] S. Samukawa and K. Tsuda, Jpn. J. Appl. Phys. **37**, L1095 (1998).
[6] S. Samukawa and T. Mukai, Proceedings of the International Symposium on Electron-Molecule Collisions and Swarms, Tokyo, Japan, 18–20 July 1999, edited by Y. Hatano, H. Tanaka, and N. Kouchi, p. 76.
[7] S. Solomon, J. B. Burkholder, A. R. Ravishankara, and R. R. Garcia, J. Geophys. Res. D: Atmos. **99**, 20929 (1994).
[8] *Climate Change 1995; The Science of Climate Change* (published for the Intergovernmental Panel on Climate Change), edited by J. T. Houghton, L. G. M. Filho, B. A. Callander, N. Harris, A. Kattenberg, and K. Maskell (Cambridge University Press, Cambridge, U. K., 1996), p. 93.
[9] O. V. Rattigan, D. E. Shallcross, and R. A. Cox, J. Chem. Soc. Faraday Trans. **93**, 2839 (1997).
[10] *Climate Change 1995; The Science of Climate Change* (published for the Intergovernmental Panel on Climate Change), edited by J. T. Houghton, L. G. M. Filho, B. A. Callander, N. Harris, A. Kattenberg, and K. Maskell (Cambridge University Press, Cambridge, U. K., 1996), p. 121.
[11] L. G. Christophorou, J. K. Olthoff, and M. V. V. S. Rao, J. Phys. Chem. Ref. Data **25**, 1341 (1996) [Electron Interactions with CF_4].
[12] L. G. Christophorou, J. K. Olthoff, and M. V. V. S. Rao, J. Phys. Chem. Ref. Data **26**, 1 (1997) [Electron Interactions with CHF_3].
[13] L. G. Christophorou, J. K. Olthoff, and Y. Wang, J. Phys. Chem. Ref. Data **26**, 1205 (1997) [Electron interactions with CCl_2F_2].
[14] L. G. Christophorou and J. K. Olthoff, J. Phys. Chem. Ref. Data **27**, 1 (1998) [Electron Interactions with C_2F_6].
[15] L. G. Christophorou and J. K. Olthoff, J. Phys. Chem. Ref. Data **27**, 889 (1998) [Electron Interactions with C_3F_8].
[16] L. G. Christophorou and J. K. Olthoff, J. Phys. Chem. Ref. Data **28**, 131 (1999) [Electron Interactions with Cl_2].
[17] L. G. Christophorou and J. K. Olthoff, J. Phys. Chem. Ref. Data **28**, 967 (1999) [Electron Interactions with Plasma Processing Gases: An update for CF_4, CHF_3, C_2F_6, and C_3F_8].
[18] L. G. Christophorou and J. K. Olthoff, J. Phys. Chem. Ref. Data **29**, 267 (2000) [Electron Interactions with SF_6].
[19] A. L. McClellan, *Tables of Experimental Dipole Moments* (W. H. Freeman and Company, San Francisco, CA, 1963), p. 36.
[20] T. Shimanouchi, J. Phys. Chem. Ref. Data **3**, 269 (1974).
[21] H. Bürger, K. Burczyk, H. Hollenstein, and M. Quack, Mol. Phys. **55**, 255 (1985).
[22] S. Roszak, W. S. Koski, J. J. Kaufman, and K. Balasubramanian, J. Chem. Phys. **106**, 7709 (1997).
[23] C. B. Leffert, Ph.D. Dissertation, Wayne State University, 1974; as quoted in Ref. 24.
[24] S. Y. Tang, B. P. Mathur, E. W. Rothe, and G. P. Reck, J. Chem. Phys. **64**, 1270 (1976).
[25] R. N. Compton, P. W. Reinhardt, and C. D. Cooper, J. Chem. Phys. **68**, 4360 (1978).
[26] P. E. McNamee, K. Lacman, and D. R. Herschbach, Faraday Discuss. Chem. Soc. **55**, 318 (1973).
[27] J. Marriott and J. D. Craggs, J. Electronics **1**, 405 (1956).
[28] C. A. Goy, A. Lord, and H. O. Pritchard, J. Phys. Chem. **71**, 1086 (1967).
[29] P. Felder, Chem. Phys. **143**, 141 (1990).
[30] H. J. M. Bowen, Trans. Faraday Soc. **50**, 444 (1954).
[31] J. Sheridan and W. Gordy, J. Chem. Phys. **20**, 591 (1952).
[32] C.-H. Wong and V. Schomaker, J. Chem. Phys. **28**, 1010 (1958).
[33] A. P. Cox, G. Duxbury, J. A. Hardy, and Y. Kawashima, J. Chem. Soc. Faraday 2 **76**, 339 (1980).
[34] V. H. Dibeler, R. M. Reese, and F. L. Mohler, J. Research NBS **57**, 113 (1956).
[35] M. Heni and E. Illenberger, Chem. Phys. Lett. **131**, 314 (1986).
[36] T. Oster, O. Ingólfsson, M. Meinke, T. Jaffke, and E. Illenberger, J. Chem. Phys. **99**, 5141 (1993).
[37] Y. Le Coat, R. Azria, M. Tronc, O. Ingólfsson, and E. Illenberger, Chem. Phys. Lett. **296**, 208 (1998).
[38] T. Underwood-Lemons, T. J. Gergel, and J. H. Moore, J. Chem. Phys. **102**, 119 (1995).
[39] I. S. Buchel'nikova, J. Exptl. Theoret. Phys. (U.S.S.R.) **35**, 1119 (1958) [Sov. Phys. JETP **8**, 783 (1959)].
[40] T. Underwood-Lemons, D. C. Winkler, J. A. Tossell, and J. H. Moore, J. Chem. Phys. **100**, 9117 (1994).
[41] I. Hahndorf and E. Illenberger, Int. J. Mass Spectrom. Ion Processes **167/168**, 87 (1997).
[42] M. Okamoto, M. Hoshino, Y. Sakamoto, S. Watanabe, M. Kitajima, H. Tanaka, and M. Kimura, Proceedings of the International Symposium on Electron-Molecule Collisions and Swarms, Tokyo, Japan, 18–20 July, 1999, edited by Y. Hatano, H. Tanaka, and N. Kouchi, p. 191.
[43] M. Kitajima, M. Okamoto, H. Tanaka, and S. Samukawa (unpublished).
[44] H. Tanaka (private Communication, January, 2000).
[45] L. Brouwer and J. Troe, Chem. Phys. Lett. **82**, 1 (1981).
[46] A. Fahr, A. K. Nayak, and R. E. Huie, Chem. Phys. **199**, 275 (1995).
[47] M. B. Robin, *Higher Excited States of Polyatomic Molecules* (Academic, New York, 1974), Vol. I.
[48] G. Herzberg, *Molecular Spectra and Molecular Structure III: Electronic Spectra and Electronic Structure of Polyatomic Molecules* (D. Van Nostrand, Princeton, N.J., 1966), p. 532.
[49] S. S. Kumaran, M.-C. Su, K. P. Lim, and J. V. Michael, Chem. Phys. Lett. **243**, 59 (1995).
[50] C. J. Noutary, J. Res. Natl. Bur. Stand. (U.S.) **72A**, 479 (1969).
[51] S. G. Lias, J. E. Bartmess, J. F. Liebman, J. L. Holmes, R. D. Levin, and W. G. Mallard, J. Phys. Chem. Ref. Data **17**(1), 60 (1988).
[52] I. Novak, as quoted in Ref. 53.
[53] L. R. Thorne and J. L. Beauchamp, J. Chem. Phys. **74**, 5100 (1981).
[54] D. W. Berman, J. L. Beauchamp, and L. R. Thorne, Int. J. Mass Spectrom. Ion Phys. **39**, 47 (1981).
[55] T. Cvitaš, H. Güsten, L. Klasinc, I. Novadj, and H. Vančik, Z. Naturforsch. **33a**, 1528 (1978).
[56] M. B. Robin, *Higher Excited States of Polyatomic Molecules* (Academic, Orlando, FL, 1985), Vol. III, p. 27.
[57] R. A. A. Boschi and D. R. Salahub, Can. J. Chem. **52**, 1217 (1974).
[58] K. B. Riehl, Ph.D. Dissertation, Air Force University, 1992; Air Force Technical Report No. AFIT/DS/ENP/92-3 (December 1992).
[59] I. Powis, O. Dutuit, M. Richard-Viard, and P. M. Guyon, J. Chem. Phys. **92**, 1643 (1990).
[60] M. K. Kawada, O. Sueoka, and M. Kimura, Chem. Phys. Lett. (to be published); M. Kimura (private communication, June 2000); M. Kimura, O. Sueoka, A. Hamada, H. Tanaka, and M. Kitajima, Bull. Am. Phys. Soc. **44**, 19 (1999).
[61] S. Altshuler, Phys. Rev. **107**, 114 (1957).
[62] L. G. Christophorou and A. A. Christodoulides, J. Phys. B **2**, 71 (1969).
[63] L. G. Christophorou, *Atomic and Molecular Radiation Physics* (Wiley-Interscience, New York, 1971), Chap. 4.
[64] C. Jiao *et al.* (2000); C. Jiao (private communication, December 1999).
[65] R. C. Wetzel, F. A. Baiocchi, T. R. Hayes, and R. S. Freund, Phys. Rev. A **35**, 559 (1987).
[66] S. R. Heller and G. W. A. Milne, Eds. EPA/NIH Mass Spectral Data Base (U.S. GPO, Washington, 1978).

[67] Z.-J. Sun, A. L. Schwaner, and J. M. White, Chem. Phys. Lett. **219**, 118 (1994).
[68] J. A. Beran and L. Kevan, J. Phys. Chem. **73**, 3866 (1969).
[69] O. Ingólfsson and E. Illenberger, Int. J. Mass Spectrom. Ion Processes **155**, 1 (1996).
[70] H. Shimamori and Y. Nakatani, Chem. Phys. Lett. **150**, 109 (1988).
[71] H. Shimamori, Y. Tatsumi, Y. Ogawa, and T. Sunagawa, J. Chem. Phys. **97**, 6335 (1992).
[72] R. G. Levy, S. J. Burns, and D. L. McFadden, Chem. Phys. Lett. **231**, 132 (1994).
[73] T. Sunagawa and H. Shimamori, Proceedings of the International Symposium on Electron-Molecule Collisions and Swarms, Tokyo, Japan, 18–20 July, 1999, edited by Y. Hatano, H. Tanaka, and N. Kouchi, p. 181.
[74] S. H. Alajajian, K.-F. Man, and A. Chutjian, J. Chem. Phys. **94**, 3629 (1991).
[75] Z. Zheng, X. Ling, K. A. Smith, and F. B. Dunning, J. Chem. Phys. **92**, 285 (1990).
[76] X. Ling, M. A. Durham, A. Kalamarides, R. W. Marawar, B. G. Lindsay, K. A. Smith, and F. B. Dunning, J. Chem. Phys. **93**, 8669 (1990).
[77] M. Suh, W. Sung, S.-U. Heo, and H. J. Hwang, J. Phys. Chem. A **103**, 8365 (1999).
[78] L. G. Christophorou and J. K. Olthoff, Adv. Atom. Mol. Opt. Phys. **44**, 155 (2000).
[79] J. H. Moore (private communication, June 2000).
[80] B. G. Zollars, C. Higgs, F. Lu, C. W. Walter, L. G. Gray, K. A. Smith, F. B. Dunning, and R. F. Stebbings, Phys. Rev. A **32**, 3330 (1985).
[81] X. Ling, B. G. Lindsay, K. A. Smith, and F. B. Dunning, Phys. Rev. A **45**, 242 (1992).
[82] F. B. Dunning, J. Phys. B **28**, 1645 (1995).
[83] J. Sherwell, R. Cooper, D. C. Nguyen, and S. P. Mezyk, Aust. J. Chem. **41**, 1491 (1988).
[84] R. Martínez, J. Terrón, I. Merelas, M. N. S. Rayo, and F. Castaño, J. Phys. B **31**, 1793 (1998).